Synthesis, molecular modeling, and biological evaluation of cinnamic acid metronidazole ester derivatives as novel anticancer agents

Yong Qian, Hong-Jia Zhang, Hao Zhang, Chen Xu *, Jing Zhao *, Hai-Liang Zhu *

State Key Laboratory of Pharmaceutical Biotechnology, Nanjing University, Nanjing 210093, People's Republic of China

ARTICLE INFO

ABSTRACT

A series of novel cinnamic acid metronidazole ester derivatives have been designed and synthesized, and their biological activities were also evaluated as potential EGFR and HER-2 kinase inhibitors. Compound **3h** showed the most potent biological activity (IC$_{50}$ = 0.62 μM for EGFR and IC$_{50}$ = 2.15 μM for HER-2). Docking simulation was performed to position compound **3h** into the EGFR active site to determine the probable binding model. Antiproliferative assay results demonstrated that some of these compounds possessed good antiproliferative activity against MCF-7. Compound **3h** with potent inhibitory activity in tumor growth inhibition may be a potential anticancer agent.

1. Introduction

Angiogenesis has been intensely investigated as an attractive cancer therapeutic target during the last decade, as angiogenesis is the first rate-limiting step for tumor cells to metastasize and is also essential for cancer growth.[1] The rapid progression of this field is that some important receptors involved in angiogenesis have been identified, including vascular endothelial growth factor receptor (VEGFR), epidermal growth factor receptor (EGFR), and several others.[2] These growth factor receptor kinases play important roles in the development, progression, aggressiveness, and metastasis of many solid tumors, such as non small cell lung cancer,[3] head and neck cancers,[4] and glioblastomas.[5] Among these kinases, EGFR (also known as erbB-1 or HER-1) and the related human epidermal growth factor receptor HER-2 (also known as erbB-2) that have been improved to be relevant for cancer. Erlotinilb inhibits EGFR that is overexpressed in tumors and is approved antitumor agent.[6] Thus, these factors are important targets for the development of new therapeutic antitumor agents.[7,8]

Nitroimidazoles have been extensively used as antimicrobial chemotherapeutics and as antiangiogenic hypoxic cell radiosensitizers.[9] Nitroimidazole derivatives have attracted considerable attention as they showed a tendency to penetrate and accumulate in regions of tumors,[10–12] and can undergo bioreduction to yield electrophilic substances which can damage protein and nucleic acids.[13] Importantly, the toxicology and metabolism of nitroimidazoles, particularly metronidazole, have been characterized.[14,15]

So nitroimidazoles may provide the attractive possibility of employing these molecules as carriers for targeted delivery in cancer therapy.[12,16] Recently, Swenson et al. synthesized a [10]B-enriched nitroimidazole by coupling the Cs salt of BSH (Cs$_2$-[10]B$_{12}$-H$_{11}$SH) with 1-(2-bromoethyl)-2-methyl-5-nitroimidazole and used for boron neutron capture therapy of cancer.[17]

As a novel class of bioreductively activated nitroimidazole compounds, we designed and synthesized a series of cinnamic acid metronidazole ester derivatives. We chose cinnamoyl moiety as it was found in a variety of biologically active substances.[18,19] Antitumor activities of various cinnamic acid derivatives were also explored by many research groups. Particularly, cinnamic acid ester derivatives shown the potential antitumor activity.[20–22] In this study, we described the synthesis and the SAR of the novel series of cinnamic acid metronidazole ester derivatives, and the biological activity evaluation indicated that some of these compounds are potent inhibitors of EGFR and HER-2. Docking simulations were performed using the X-ray crystallographic structure of the EGFR in complex with an inhibitor to explore the binding modes of these compounds at the active site.

2. Results and discussion

2.1. Chemistry

The synthetic route for the novel cinnamic acid metronidazole ester derivatives **3a–s** is outlined in Scheme 1. These compounds were synthesized from cinnamic acids (**1**) and active metronidazone (**2**). Compound (**1**) was prepared according the modified procedure of Davis et al.[23] Aromatic aldehydes and malonic acid were

* Corresponding authors. Tel./fax: +86 25 8359 2572.
  E-mail address: zhuhl@nju.edu.cn (H.-L. Zhu).
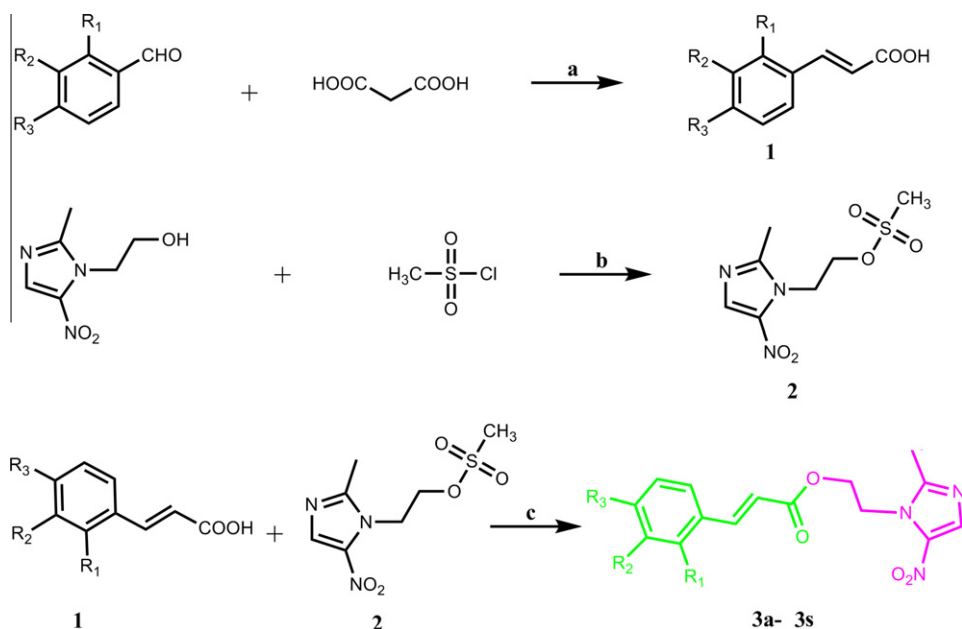
Scheme 1. General synthesis of cinnamic acid metronidazole ester derivatives (**3a–s**). Reagents and conditions: (a) piperidine, pyridine, 80–90 °C, 24 h; (b) CH₂Cl₂, NEt₃; (c) K₂CO₃, DMF, 80 °C, 24 h.

dissolved in a mixture of pyridine and piperidine and refluxed for 24 h, and cinnamic acids were obtained with yields of 75–85%. Then, cinnamic acids (**1**), active metronidazole (**2**) and K_2CO_3 were taken in DMF and refluxed to provide the desired compounds (**3a–s**) (Table 1). All of the synthetic compounds gave satisfactory analytical and spectroscopic data, which were in full accordance with their depicted structures.
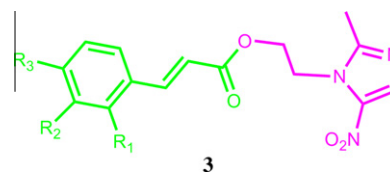
2.2. Biological activity

All the synthesized cinnamic acid metronidazole ester derivatives were evaluated for their ability to inhibit the autophosphorylation of EGFR and HER-2 kinases using a solid-phase ELISA assay. The results were summarized in Table 2. For the given compounds, it was observed that the IC_{50} value for inhibition of HER-2 kinase was higher than that observed of EGFR kinase, however, they had the same trends. It was possibly attributed to the fact that higher concentration of the purified HER-2 kinase was used than EGFR kinase in the enzyme assays. It is evident that there is also a reasonable correlation between the EGFR and HER-2 inhibitory activities; thus, this is not surprising in view of the high sequence homology of the catalytic domains of these two kinases. As shown in Table 2, a number of cinnamic acid metronidazole ester derivatives exhibited significant EGFR and HER-2 inhibitory activity. Among them, compound **3h** displayed the most potent inhibitory activity ($IC_{50} = 0.62$ μM for EGFR and $IC_{50} = 2.15$ μM for HER-2), comparable to the positive control erlotinib ($IC_{50} = 0.03$ μM for EGFR).

Structure–activity relationships in these cinnamic acid metronidazole ester derivatives demonstrated that compounds with substitution at the *meta* (**3o–q**) or *para* (**3a–i**) position showed more potent activities than those with substitution at the *ortho* position (**3j–n**). A comparison of the *para* position substitution on benzene ring demonstrated that a *para* halogen group (**3a–c**) may have more slightly improved EGFR inhibitory activity and the potency order is F < Cl < Br, and other *para* substituents prepared (**3e**, **3g**) had minimal effects compared with **3d**, whereas a methoxy group substituent (**3f**) led to a slight loss of activity. Meanwhile, a significant loss of activity was observed when the halogen substituent was moved from the *para* position to the *ortho* (**3j–m**) position.

Table 1
Structure of cinnamic acid metronidazole ester derivatives (**3a–s**)

Compound	R₁	R₂	R₃
3a	H	H	F
3b	H	H	Cl
3c	H	H	Br
3d	H	H	H
3e	H	H	Me
3f	H	H	OMe
3g	H	H	i-Pr
3h	H	H	Ph
3i	H	H	PhCH₂O
3j	F	H	H
3k	Cl	H	H
3l	Br	H	H
3m	NO₂	H	H
3n	OMe	H	H
3o	H	NO₂	H
3p	H	F	H
3q	H	OMe	H

Table 2
Inhibition (IC$_{50}$) of EGFR and HER-2 kinases and inhibition (IC$_{50}$) of cell proliferation by compound **3a–s**

| Compounds	Enzyme assay IC$_{50}$ (μM)		MCF-7 IC$_{50}$ ± SD (μM)
	EGFR	HER-2	
3a	4.12	5.84	3.76 ± 0.12
3b	3.62	4.77	3.05 ± 0.15
3c	3.24	4.65	2.45 ± 0.08
3d	7.83	10.78	4.41 ± 0.3
3e	8.11	9.65	4.28 ± 0.5
3f	10.85	14.32	5.49 ± 0.2
3g	6.82	9.97	4.96 ± 0.4
3h	0.62	2.15	0.36 ± 0.04
3i	1.27	3.46	0.98 ± 0.06
3j	26.74	41.26	15 ± 2
3k	20.81	36.45	18 ± 4
3l	24.32	44.85	16 ± 3
3m	25	40	17 ± 3
3n	32	>50	20 ± 2
3o	14.53	19.34	5.68 ± 0.4
3p	12.42	16.75	5.88 ± 0.8
3q	13.87	18.82	5.75 ± 0.7
3r	3.88	5.03	3.4 ± 0.2
3s	5.76	9.24	4.1 ± 0.3
Erlotinib	0.03	0.16	0.02 ± 0.005

A methoxy group at *ortho* position in the **3n** structure also led to a noteworthy loss of activity. Considering the steric effect of the substitution at the *para* position of benzene ring, we designed and evaluated the compounds with phenyl (**3h**) or benzyloxy (**3i**) group substitution, the activity was significantly enhanced up to 12-fold and 4.5-fold by phenyl and benzyloxy group substituent, respectively, which was compared with the compound **3d**. Furthermore, variation of the aromatic ring moiety was also explored. Compounds **3r** and **3s** bearing naphthyl moiety exhibited moderate EGFR inhibitory activity.

In order to gain more understanding of the structure–activity relationships observed at the EGFR, molecular docking of the most potent inhibitor **3h** into ATP binding site of EGFR kinase was performed on the binding model based on the EGFR complex structure (1M17.pdb). The binding model of compound **3h** and EGFR is depicted in Figure 1. In the binding model, compound **3h** is nicely bound to the region with the carbonyl group project toward the amino hydrogen of Lys828, and the oxygen atom of ester group of **3h** also forms hydrogen bond with the hydroxyl group Leu768, and oxygen atom of nitro group with amino hydrogen of Lys822. The enzyme assay data and the molecular docking results showed that compound **3h** was a potential inhibitor of EGFR (Fig. 1).
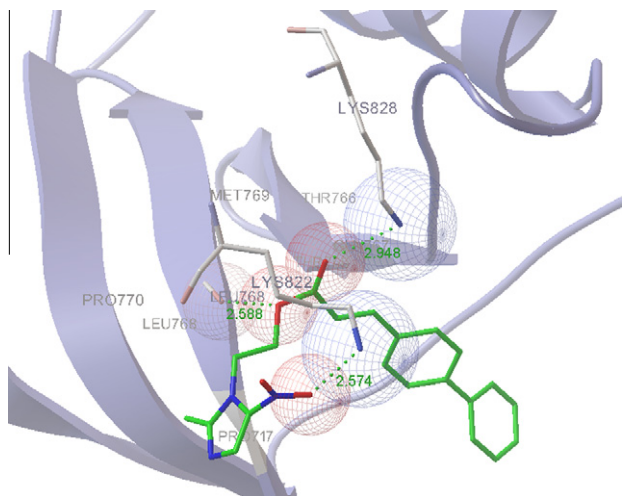
Figure 1. Docking of compound **3h** with EGFR kinase shows intramolecular hydrogen bonds with Lys828, Leu768, and Lys822.
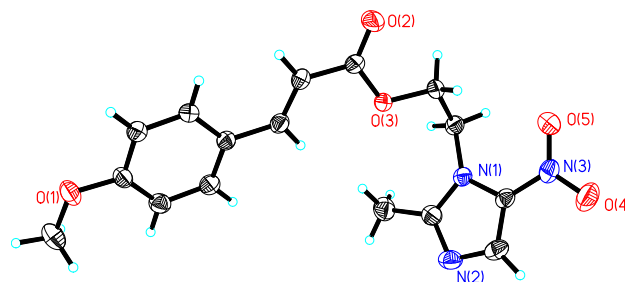
Figure 2. Crystal structure diagrams of compound **3f**. Molecule structure diagram with displacement ellipsoids being at the 30% probability level and H atoms are shown as small spheres of arbitrary radii.

In addition, in vitro antiproliferative activity of these cinnamic acid metronidazole ester derivatives was studied on a panel of one human tumor cell line (MCF-7), which overexpressed EGFR and to a less extent, HER-2. Compounds **3b**, **3c**, **3h**, **3i**, **3r**, which have potent inhibitory activity of EGFR and HER-2 showed high antiproliferative activity against MCF-7 with IC$_{50}$ ranging from 0.36 ± 0.04 μM to 3.4 ± 0.2 μM, which indicated that these cinnamic acid metronidazole ester derivatives were potent inhibitor of EGFR and HER-2 as antitumor agents. Among these compounds, compound **3h** exhibited the most potential inhibitory activity in tumor growth inhibition and exhibited favored EGFR and HER-2 inhibitory activity.

3. Conclusions

A series of cinnamic acid metronidazole ester derivatives have been designed and synthesized, and their biological activities were also evaluated as potent EGFR and HER-2 inhibitory. Compound **3h** demonstrated the most potent inhibitory activity (IC$_{50}$ = 0.62 μM for EGFR and IC$_{50}$ = 2.15 μM for HER-2), which was compared with the positive control erlotinib. Docking simulation was performed to position compound **3h** into the EGFR active site to determine the probable binding model. Analysis of the compound **3h**'s binding conformation in active site displayed the compound **3h** was stabilized by hydrogen bonding interactions with Lys828, Leu768, and Lys822. Antiproliferative assay results also showed that these cinnamic acid metronidazole ester derivatives had the potential to be developed for antiproliferative agents against MCF-7. Particularly, compound **3h** has demonstrated significant EGFR and HER-2 and tumor growth inhibitory activity as a potential anticancer agent.

4. Experiments

4.1. Materials and measurements

All chemicals and reagents used in current study were analytical grade. All the ^{1}H NMR spectra were recorded on a Bruker DRX 500 or DPX 300 model spectrometer in CDCl$_3$ and chemical shifts were reported in ppm (δ). ESI-MS spectra were recorded on a Mariner System 5304 Mass spectrometer. Elemental analyses were performed on a CHN-O-Rapid instrument. TLC was performed on the glass-backed silica gel sheets (Silica Gel 60 Å GF254) and visualized in UV light (254 nm). Column chromatography was performed using silica gel (200–300 mesh) eluting with ethyl acetate and petroleum ether.

4.2. General procedure for synthesis of cinnamic acids

A mixture of aromatic aldehydes (3.2 mmol), malonic acid (3.87 mmol), piperidine (0.387 mmol) was dissolved in pyridine

and stirred on 80–90 °C for 24 h. The pyridine was removed at the vacuum. The reaction mixture was poured in water and washed with HCl, the precipitate was filtered and washed with hexane about three times, and dried under vacuum to afford the cinnamic acids (Scheme 1).

4.3. General procedure for synthesis of 2-(2-methyl-5-nitro-1*H*-imidazol-1-yl) ethyl methanesulfonate

Equimolar amount of metronidazole and methanesulfonyl chloride were dissolved in dichloromethane, triethylamine as a catalyst and stirred in the ice bath for 5 h. The reaction mixture was extracted with ice water and saturated sodium bicarbonate, respectively. Then, the organic layer was collected and crystallized to get the product (Scheme 1).

4.4. General procedure for synthesis of cinnamic acid metronidazole ester derivatives

To a stirred solution of cinnamic acids (0.5 mmol), 2-(2-methyl-5-nitro-1*H*-imidazol-1-yl) ethyl methanesulfonate (0.5 mmol) in DMF, potassium carbonate (1 mmol) was added. This mixture was stirred at 80 °C for 24 h. Then the mixture was filtered and the filtrate was taken up with EtOAc, washed with saturated sodium bicarbonate, dried over Na_2SO_4, and purified by column chromatography on silica gel, to give the target compounds (Scheme 1).

4.4.1. (*E*)-2-(2-Methyl-5-nitro-1*H*-imidazol-1-yl)ethyl 3-(4-fluorophenyl) acrylate (3a)

^{1}H NMR (CDCl$_3$, 500 MHz): 2.52 (s, 3H), 4.55 (t, *J* = 5.2 Hz, 2H), 4.66 (t, *J* = 5.2 Hz, 2H), 6.26 (d, *J* = 16.0 Hz, 1H), 7.01 (t, *J* = 8.5 Hz, 2H), 7.49–7.51 (m, 2H), 7.61 (d, *J* = 15.9 Hz, 1H), 7.98 (s, 1H). ESI-MS: 320.1 (C$_{15}$H$_{15}$FN$_3$O$_4$, [M+H]$^+$). Anal. Calcd for C$_{15}$H$_{14}$FN$_3$O$_4$: C, 56.43; H, 4.42; N, 13.16. Found: C, 55.77; H, 4.78; N, 13.49.

4.4.2. (*E*)-2-(2-Methyl-5-nitro-1*H*-imidazol-1-yl)ethyl 3-(4-chlorophenyl) acrylate (3b)

^{1}H NMR (CDCl$_3$, 300 MHz): 2.52 (s, 3H), 4.56 (t, *J* = 4.9 Hz, 2H), 4.66 (t, *J* = 4.9 Hz, 2H), 6.31 (d, *J* = 16.1 Hz, 1H), 7.37 (d, *J* = 8.4 Hz, 2H), 7.45 (d, *J* = 8.4 Hz, 2H), 7.60 (d, *J* = 15.9 Hz, 1H), 7.98 (s, 1H). ESI-MS: 336.1 (C$_{15}$H$_{15}$ClN$_3$O$_4$, [M+H]$^+$). Anal. Calcd for C$_{15}$H$_{14}$ClN$_3$O$_4$: C, 53.66; H, 4.20; N, 12.52. Found: C, 53.98; H, 4.61; N, 12.84.

4.4.3. (*E*)-2-(*2-Methyl-5-nitro-1H*-imidazol-1-yl)ethyl 3-(4-bromophenyl) acrylate (3c)

^{1}H NMR (CDCl$_3$, 300 MHz): 2.52 (s, 3H), 4.55 (t, *J* = 4.9 Hz, 2H), 4.67 (t, *J* = 4.9 Hz, 2H), 6.32 (d, *J* = 15.9 Hz, 1H), 7.37 (d, *J* = 8.6 Hz, 2H), 7.52–7.61 (m, 3H), 7.98 (s, 1H). ESI-MS: 380.0 (C$_{15}$H$_{15}$BrN$_3$O$_4$, [M+H]$^+$). Anal. Calcd for C$_{15}$H$_{14}$BrN$_3$O$_4$: C, 47.39; H, 3.71; N, 11.05. Found: C, 47.70; H, 4.03; N, 11.38.

4.4.4. (*E*)-2-(2-Methyl-5-nitro-1*H*-imidazol-1-yl)ethyl cinnamate (3d)

^{1}H NMR (CDCl$_3$, 300 MHz): 2.55 (s, 3H), 4.57 (t, *J* = 4.8 Hz, 2H), 4.67 (t, *J* = 5.1 Hz, 2H), 6.34 (d, *J* = 16.1 Hz, 1H), 7.40–7.42 (m, 3H), 7.50–7.53 (m, 2H), 7.67 (d, *J* = 15.9 Hz, 1H), 8.00 (s, 1H). ESI-MS: 302.1 (C$_{15}$H$_{16}$N$_3$O$_4$, [M+H]$^+$). Anal. Calcd for C$_{15}$H$_{15}$N$_3$O$_4$: C, 59.79; H, 5.02; N, 13.95. Found: C, 60.14; H, 5.39; N, 14.41.

4.4.5. (*E*)-2-(2-Methyl-5-nitro-1*H*-imidazol-1-yl)ethyl 3-*p*-tolyl-acrylate (3e)

^{1}H NMR (CDCl$_3$, 500 MHz): 2.38 (s, 3H), 2.52 (s, 3H), 4.55 (m, 2H), 4.66 (m, 2H), 6.29 (d, *J* = 15.8 Hz, 1H), 7.20 (d, *J* = 7.8 Hz, 2H), 6.40 (d, *J* = 8.0 Hz, 2H), 7.62 (d, *J* = 15.8 Hz, 1H), 7.99 (s, 1H). ESI-MS: 316.1 (C$_{16}$H$_{18}$N$_3$O$_4$, [M+H]$^+$). Anal. Calcd for C$_{16}$H$_{17}$N$_3$O$_4$: C, 60.94; H, 5.43; N, 13.33. Found: C, 61.33; H, 5.79; N, 13.65.

4.4.6. (*E*)-2-(2-Methyl-5-nitro-1*H*-imidazol-1-yl)ethyl 3-(4-methoxyphenyl) acrylate (3f)

^{1}H NMR (CDCl$_3$, 500 MHz): 2.52 (s, 3H), 3.84 (s, 3H), 4.54 (t, *J* = 4.8 Hz, 2H), 4.65 (t, *J* = 5.2 Hz, 2H), 6.20 (d, *J* = 15.8 Hz, 1H), 6.91 (d, *J* = 8.5 Hz, 2H), 7.46 (d, *J* = 8.8 Hz, 2H), 7.61 (d, *J* = 16.2 Hz, 1H), 7.98 (s, 1H). ESI-MS: 332.1 (C$_{16}$H$_{18}$N$_3$O$_5$, [M+H]$^+$). Anal. Calcd for C$_{16}$H$_{17}$N$_3$O$_5$: C, 58.00; H, 5.17; N, 12.68. Found: C, 58.33; H, 5.43; N, 12.95.

4.4.7. (*E*)-2-(2-Methyl-5-nitro-1*H*-imidazol-1-yl)ethyl 3-(4-isopropylphenyl) acrylate (3g)

^{1}H NMR (CDCl$_3$, 500 MHz): 1.26 (s, 6H), 2.55 (s, 3H), 2.89 (m, 1H), 4.56 (t, *J* = 5.5 Hz, 2H), 4.66 (t, *J* = 5.2 Hz, 2H), 6.44 (d, *J* = 16.2 Hz, 1H), 6.92 (d, *J* = 8.2 Hz, 1H), 6.95–6.98 (m, 1H), 7.37 (t, *J* = 7.0 Hz, 1H), 7.48 (d, *J* = 6.2 Hz, 1H), 7.95–7.98 (d, *J* = 16.2 Hz, 1H), 7.99 (s, 1H). ESI-MS: 344.2 (C$_{18}$H$_{22}$N$_3$O$_4$, [M+H]$^+$). Anal. Calcd for C$_{18}$H$_{21}$N$_3$O$_4$: C, 62.96; H, 6.16; N, 12.24. Found: C, 63.31; H, 6.48; N, 12.58.

4.4.8. (*E*)-2-(2-Methyl-5-nitro-1*H*-imidazol-1-yl)ethyl 3-(4-phenyl) acrylate (3h)

^{1}H NMR (CDCl$_3$, 300 MHz): 2.56 (s, 3H), 4.58 (t, *J* = 4.9 Hz, 2H), 4.66 (t, *J* = 5.1 Hz, 2H), 6.37 (d, *J* = 16.1 Hz, 1H), 7.39 (d, *J* = 7.1 Hz, 1H), 7.46 (t, *J* = 7.1 Hz, 2H), 7.57–7.65 (m, 6H), 7.70 (d, *J* = 15.9 Hz, 1H), 7.99 (s, 1H). ESI-MS: 378.1 (C$_{21}$H$_{20}$N$_3$O$_4$, [M+H]$^+$). Anal. Calcd for C$_{21}$H$_{19}$N$_3$O$_4$: C, 66.83; H, 5.07; N, 11.13. Found: C, 67.14; H, 5.39; N, 11.48.

4.4.9. (*E*)-2-(2-Methyl-5-nitro-1*H*-imidazol-1-yl)ethyl 3-(4-(benzyloxy) phenyl) acrylate (3i)

^{1}H NMR (CDCl$_3$, 500 MHz): 2.58 (s, 3H), 4.64 (t, *J* = 5.0 Hz, 2H), 4.72 (t, *J* = 5.0 Hz, 2H), 5.18 (s, 2H), 7.10 (d, *J* = 8.5 Hz, 1H), 7.29–7.47 (m, 7H), 7.71 (d, *J* = 8.0 Hz, 2H), 7.86 (d, *J* = 8.5 Hz, 1H), 8.01 (s, 1H). ESI-MS: 407.1 (C$_{22}$H$_{22}$N$_3$O$_5$, [M+H]$^+$). Anal. Calcd for C$_{22}$H$_{21}$N$_3$O: C, 64.86; H, 5.20; N, 10.31. Found: C, 65.23; H, 5.47; N, 10.65.

4.4.10. (*E*)-2-(2-Methyl-5-nitro-1*H*-imidazol-1-yl)ethyl 3-(2-fluorophenyl) acrylate (3j)

^{1}H NMR (CDCl$_3$, 300 MHz): 2.52 (s, 3H), 4.58 (t, *J* = 5.0 Hz, 2H), 4.66 (t, *J* = 4.9 Hz, 2H), 6.26 (d, *J* = 16.1 Hz, 1H), 7.09 (t, *J* = 8.6 Hz, 2H), 7.48–7.53 (m, 2H), 7.61 (d, *J* = 15.9 Hz, 1H), 7.98 (s, 1H). ESI-MS: 320.1 (C$_{15}$H$_{15}$FN$_3$O$_4$, [M+H]$^+$). Anal. Calcd for C$_{15}$H$_{14}$FN$_3$O$_4$: C, 56.43; H, 4.42; N, 13.16. Found: C, 56.74; H, 4.77; N, 13.45.

4.4.11. (*E*)-2-(2-Methyl-5-nitro-1*H*-imidazol-1-yl)ethyl 3-(2-chlorophenyl) acrylate (3k)

^{1}H NMR (CDCl$_3$, 300 MHz): 2.55 (s, 3H), 4.58 (t, *J* = 4.9 Hz, 2H), 4.67 (t, *J* = 4.9 Hz, 2H), 6.35 (d, *J* = 16.1 Hz, 1H), 7.27–7.36 (m, 2H), 7.43 (d, *J* = 1.7 Hz, *J* = 7.9 Hz, 1H), 7.59 (dd, *J* = 2.0 Hz, *J* = 7.3 Hz, 1H), 7.98 (s, 1H), 8.05 (d, *J* = 15.9 Hz, 1H). ESI-MS: 336.1 (C$_{15}$H$_{15}$ClN$_3$O$_4$, [M+H]$^+$). Anal. Calcd for C$_{15}$H$_{14}$ClN$_3$O$_4$: C, 53.66; H, 4.20; N, 12.52. Found: C, 53.96; H, 4.55; N, 12.86.

4.4.12. (*E*)-2-(2-Methyl-5-nitro-1*H*-imidazol-1-yl)ethyl 3-(2-bromophenyl)acrylate (3l)

^{1}H NMR (CDCl$_3$, 300 MHz): 2.52 (s, 3H), 4.56 (t, *J* = 4.9 Hz, 2H), 4.64 (t, *J* = 4.9 Hz, 2H), 6.37 (d, *J* = 16.1 Hz, 1H), 7.29–7.35 (m, 2H), 7.44 (d, *J* = 2.0 Hz, *J* = 7.8 Hz, 1H), 7.60 (m, 1H), 7.99 (s, 1H), 8.04 (d, *J* = 16.1 Hz, 1H). ESI-MS: 379.0 (C$_{15}$H$_{15}$BrN$_3$O$_4$, [M+H]$^+$). Anal. Calcd for C$_{15}$H$_{14}$BrN$_3$O$_4$: C, 47.39; H, 3.71; N, 11.05. Found: C, 47.76; H, 4.05; N, 11.36.

4.4.13. (E)-2-(2-Methyl-5-nitro-1H-imidazol-1-yl)ethyl 3-(2-nitrophenyl)acrylate (3m)

^{1}H NMR (CDCl$_3$, 500 MHz): 2.57 (s, 3H), 4.61 (t, J = 5.0 Hz, 2H), 4.69 (t, J = 5.0 Hz, 2H), 6.28 (d, J = 15.5 Hz, 1H), 7.58–7.63 (m, 2H), 7.69 (d, J = 7.0 Hz, 2H), 7.99 (s, 1H), 8.09 (d, J = 9.5 Hz, 1H), 8.13 (s, 1H). ESI-MS: 346.1 (C$_{15}$H$_{15}$N$_4$O$_6$, [M+H]$^+$). Anal. Calcd for C$_{15}$H$_{14}$N$_4$O$_6$: C, 52.03; H, 4.07; N, 16.18. Found: C, 52.34; H, 4.45; N, 16.55.

4.4.14. (E)-2-(2-Methyl-5-nitro-1H-imidazol-1-yl)ethyl 3-(2-methoxyphenyl) acrylate (3n)

^{1}H NMR (CDCl$_3$, 300 MHz): 2.56 (s, 3H), 3.89 (s, 3H), 4.57 (t, J = 4.6 Hz, 2H), 4.67 (t, J = 4.4 Hz, 2H), 6.43 (d, J = 16.1 Hz, 1H), 6.91–6.99 (m, 2H), 7.35–7.41 (m, 1H), 7.49 (dd, J = 1.65 Hz, J = 7.7 Hz, 1H), 7.96 (d, J = 16.3 Hz, 1H), 8.00 (s, 1H). ESI-MS: 332.1 (C$_{16}$H$_{18}$N$_3$O$_5$, [M+H]$^+$). Anal. Calcd for C$_{16}$H$_{17}$N$_3$O$_5$: C, 58.00; H, 5.17; N, 12.68. Found: C, 58.37; H, 5.45; N, 12.93.

4.4.15. (E)-2-(2-Methyl-5-nitro-1H-imidazol-1-yl)ethyl 3-(3-nitrophenyl) acrylate (3o)

^{1}H NMR (CDCl$_3$, 300 MHz): 2.63 (s, 3H), 4.57 (t, J = 5.0 Hz, 2H), 4.70 (t, J = 5.0 Hz, 2H), 6.20 (d, J = 15.9 Hz, 1H), 6.92 (d, J = 8.8 Hz, 2H), 7.48 (d, J = 8.8 Hz, 2H), 7.63 (d, J = 16.1 Hz, 1H), 8.04 (s, 1H). ESI-MS: 347.1 (C$_{15}$H$_{15}$N$_4$O$_6$, [M+H]$^+$). Anal. Calcd for C$_{15}$H$_{14}$N$_4$O$_6$: C, 52.03; H, 4.07; N, 16.18. Found: C, 52.36; H, 4.35; N, 16.43.

4.4.16. (E)-2-(2-Methyl-5-nitro-1H-imidazol-1-yl)ethyl 3-(3-fluorophenyl)acrylate (3p)

^{1}H NMR (CDCl$_3$, 500 MHz): 2.54 (s, 3H), 4.58 (t, J = 5.0 Hz, 2H), 4.67 (t, J = 5.0 Hz, 2H), 6.29 (d, J = 16.0 Hz, 1H), 7.13 (t, J = 8.2 Hz, 2H), 7.51–7.61 (m, 2H), 7.65 (d, J = 16.0 Hz, 1H), 7.99 (s, 1H). ESI-MS: 320.1 (C$_{15}$H$_{15}$FN$_3$O$_4$, [M+H]$^+$). Anal. Calcd for C$_{15}$H$_{14}$FN$_3$O$_4$: C, 56.43; H, 4.42; N, 13.16. Found: C, 56.80; H, 4.79; N, 13.53.

4.4.17. (E)-2-(2-Methyl-5-nitro-1H-imidazol-1-yl)ethyl 3-(3-methoxyphenyl)acrylate (3q)

^{1}H NMR (CDCl$_3$, 500 MHz): 2.55 (s, 3H), 3.86 (s, 3H), 4.58 (t, J = 5.0 Hz, 2H), 4.68 (t, J = 5.0 Hz, 2H), 6.35 (d, J = 16.0 Hz, 1H), 6.35 (dd, J = 2.0 Hz, J = 8.0 Hz, 1H), 7.04 (s, 1H), 7.12 (d, J = 8.0 Hz, 2H), 7.33 (t, J = 8.0 Hz, 1H), 7.64 (d, J = 16.0 Hz, 1H), 8.01 (s, 1H). ESI-MS: 332.1 (C$_{16}$H$_{18}$N$_3$O$_5$, [M+H]$^+$). Anal. Calcd for C$_{16}$H$_{17}$N$_3$O$_5$: C, 58.00; H, 5.17; N, 12.68. Found: C, 58.36; H, 5.52; N, 12.99.

4.4.18. (E)-2-(2-Methyl-5-nitro-1H-imidazol-1-yl)ethyl 3-(naphthalen-1-yl) acrylate (3r)

^{1}H NMR (CDCl$_3$, 500 MHz): 2.56 (s, 3H), 4.61 (t, J = 5.2 Hz, 2H), 4.70 (t, J = 5.2 Hz, 2H), 6.45 (d, J = 15.5 Hz, 1H), 7.49 (t, J = 7.5 Hz, 1H), 7.53–7.56 (m, 1H), 7.58–7.61 (m, 1H), 7.74 (d, J = 7.3 Hz, 1H), 7.89 (d, J = 8.0 Hz, 1H), 7.93 (d, J = 8.2 Hz, 1H), 8.00 (s, 1H), 8.14 (d, J = 8.2 Hz, 1H), 8.51 (d, J = 15.8 Hz, 1H). ESI-MS: 352.1 (C$_{19}$H$_{18}$N$_3$O$_4$, [M+H]$^+$). Anal. Calcd for C$_{19}$H$_{17}$N$_3$O$_4$: C, 64.95; H, 4.88; N, 11.96. Found: C, 65.30; H, 4.69; N, 12.28.

4.4.19. (E)-2-(2-Methyl-5-nitro-1H-imidazol-1-yl)ethyl 3-(naphthalen-2-yl) acrylate (3s)

^{1}H NMR (CDCl$_3$, 500 MHz): 2.56 (s, 3H), 4.59 (t, J = 5.0 Hz, 2H), 4.68 (t, J = 5.0 Hz, 2H), 6.47 (d, J = 16.0 Hz, 1H), 7.53–7.56 (m, 2H), 7.65 (d, J = 8.5 Hz, 1H), 7.82–7.89 (m, 4H), 7.94 (s, 1H), 8.01 (s, 1H). ESI-MS: 352.1 (C$_{19}$H$_{18}$N$_3$O$_4$, [M+H]$^+$). Anal. Calcd for C$_{19}$H$_{17}$N$_3$O$_4$: C, 64.95; H, 4.88; N, 11.96. Found: C, 64.96; H, 5.07; N, 12.31.

4.5. Crystal structure determination

Crystal structure determination of compound **3f** were carried out on a Nonius CAD4 diffractometer equipped with graphite-monochromated MoKα (λ = 0.71073 Å) radiation (Fig. 2). The structure was solved by direct methods and refined on F2 by full-matrix least-squares methods using SHELX-97.[24] All the non-hydrogen atoms were refined anisotropically. All the hydrogen atoms were placed in calculated positions and were assigned fixed isotropic thermal parameters at 1.2 times the equivalent isotropic U of the atoms to which they are attached and allowed to ride on their respective parent atoms. The contributions of these hydrogen atoms were included in the structure-factors calculations. The crystal data, data collection, and refinement parameter for the compound **3f** are listed in Table 3.

4.6. General procedure for preparation, purification of HER-2 and EGFR, and inhibitory assay

A 1.7 Kb cDNA encoded for human HER-2 cytoplasmic domain (HER-2-CD, amino acids 676–1245) and 1.6 kb cDNA encoded for the EGFR cytoplasmic domain (EGFR-CD, amino acids 645–1186) were cloned into baculoviral expression vectors pBlueBacHis2B and pFASTBacHTc (Huakang Company, China), separately. A sequence that encodes (His)$_6$ was located at the 5′ upstream to the HER-2 and EGFR sequences. Sf-9 cells were infected for 3 days for protein expression. Sf-9 cell pellets were solubilized at 0 °C in a buffer at pH 7.4 containing 50 mM HEPES, 10 mM NaCl, 1% Triton, 10 μM ammonium molybdate, 100 μM sodium vanadate, 10 μg/mL aprotinin, 10 μg/mL leupeptin, 10 μg/mL pepstatin, and 16 μg/mL benzamidine HCl for 20 min followed by 20 min centrifugation. Crude extract supernatant was passed through an equilibrated Ni-NTA superflow packed column and washed with 10 mM and then 100 mM imidazole to remove nonspecifically bound material. Histidine tagged proteins were eluted with 250 and 500 mM imidazole and dialyzed against 50 mM NaCl, 20 mM HEPES, 10% glycerol, and 1 μg/mL each of aprotinin, leupeptin, and pepstatin for 2 h. The entire purification procedure was performed at 4 °C or on ice.[25]

Both EGFR and HER-2 kinase assays were set up to assess the level of autophosphorylation based on DELFIA/Time-Resolved Fluorometry. Compounds **3a–s** were dissolved in 100% DMSO and diluted to the appropriate concentrations with 25 mM HEPES at pH 7.4. In each well, 10 μL compound was incubated with 10 μL (12.5 ng for HER-2 or 5 ng for EGFR) recombinant enzyme (1:80 dilution in 100 mM HEPES) for 10 min at room temperature. Then, 10 μL of 5× buffer (containing 20 mM HEPES, 2 mM MnCl$_2$, 100 μM Na$_3$VO$_4$, and 1 mM DTT) and 20 μL of 0.1 mM ATP–50 mM MgCl$_2$ were added for 1 h. Positive and negative controls were included in each plate by incubation of enzyme with or without ATP–MgCl$_2$.

Table 3
Crystallographical and experimental data for compound **3f**

Compounds	**3f**
Empirical formula	C$_{16}$H$_{17}$N$_3$O$_5$
Formula weight	331.33
Crystal system	Triclinic
Space group	p-1
a (Å)	7.7630(16)
b (Å)	8.7390(17)
c (Å)	13.290(3)
α (°)	80.94(3)
β (°)	78.11(3)
γ (°)	64.90(3)
V (Å)	796.4(3)
Z	2
D$_{calcd}$/g cm^{-3}	1.382
θ range (°)	1.57–25.27
F(000)	348
Reflections collected/unique	3126/2894 [R_{int} = 0.0287]
Data/restraints/parameters	2894/0/218
Absorption coefficient (mm^{-1})	0.104
R_1; wR_2 [I > 2σ(I)]	0.0500/0.1125
R_1; wR_2 (all data)	0.0817/0.1286
GOOF	1.019

At the end of incubation, liquid was aspirated, and plates were washed three times with wash buffer. A 75 μL (400 ng) sample of europium labeled anti-phosphotyrosine antibody was added to each well for another 1 h of incubation. After washing, enhancement solution was added and the signal was detected by Victor (Wallac Inc.) with excitation at 340 nm and emission at 615 nm. The percentage of autophosphorylation inhibition by the compounds was calculated using the following equation: $100\% - [(\text{negative control})/(\text{positive control} - \text{negative control})]$. The IC_{50} was obtained from curves of percentage inhibition with eight concentrations of compound. As the contaminants in the enzyme preparation are fairly low, the majority of the signal detected by the anti-phosphotyrosine antibody is from EGFR or HER-2.

4.7. Cell proliferation assay

The antiproliferative activity was determined using a standard (MTT)-based colorimetric assay (Sigma). Briefly, cell lines were seeded at a density of 7×10^3 cells/well in 96-well microtiter plates (Costar). After 24 h, exponentially growing cells were exposed to the indicated compounds at final concentrations ranging from 0.1 to 100 μg/mL. After 48 h, cell survival was determined by the addition of an MTT solution (10 μL of 5 mg/mL MTT in PBS). After 4 h, 100 μL of 10% SDS in 0.01 N HCl was added, and the plates were incubated at 37 °C for a further 18 h; optical absorbance was measured at 570 nm on an LX300 Epson Diagnostic microplate reader. Survival ratios are expressed in percentages with respect to untreated cells. IC_{50} values were determined from replicates of six wells at least three independent experiments.

4.8. Molecular docking modeling

Molecular docking of compound **3h** into the three-dimensional EGFR complex structure (1M17.pdb, downloaded from the PDB) was carried out using the AutoDock software package (version 4.0) as implemented through the graphical user interface AutoDockTools (ADT 1.4.6).

Acknowledgment

References and notes

1. Cherrington, J. M.; Strawn, L. M.; Shawver, L. K. *Adv. Cancer Res.* **2000**, *20*, 1.
2. Shauver, L. K.; Lipson, K. E.; Fong, T. A. T.; McMahon, G.; Strawn, L. M. In *The New Angiotherapy*; Fan, T. P., Kohn, E. C., Eds.; Humana Press: Totowa, NJ, 2002; pp 409–452. and references cited therein.
3. Tateishi, M.; Ishida, T.; Mitsudomi, T.; Kaneko, S.; Sugimachi, K. *Cancer Res.* **1990**, *50*, 7077.
4. Fleming, T. P.; Saxena, A.; Clark, W. C.; Robertson, J. T.; Oldfield, E. H.; Aaronson, S. A.; Ali, I. U. *Cancer Res.* **1992**, *52*, 4550.
5. Shin, D. M.; Ro, J. Y.; Hong, W. K.; Hittelamn, W. N. *Cancer Res.* **1994**, *54*, 3153.
6. Cohen, R. B. *Clin. Colorectal Cancer* **2003**, *2*, 246.
7. Gangjee, A.; Li, W.; Lin, L.; Zeng, Y.; Ihnat, M.; Warnke, L. A.; Green, D. W.; Cody, V.; Pace, J.; Queener, S. F. *Bioorg. Med. Chem.* **2009**, *17*, 7324.
8. Hughes, T. V.; Xu, G.; Wetter, S. K.; Connolly, P. J.; Emanuel, S. L.; Karnachi, P.; Pollack, S. R.; Pandey, N.; Adams, M.; Sandra, M. M.; Middleton, S. A.; Greenberger, L. M. *Bioorg. Med. Chem. Lett.* **2008**, *18*, 4896.
9. (a) Lau, N. P.; Piscitelli, S. C.; Wilkes, L.; Danziger, L. H. *Clin. Pharmacokinet.* **1992**, *23*, 328; (b) Uto, Y.; Nagasawa, H.; Jin, C. Z.; Nakayama, S.; Tanaka, A.; Kiyoi, S.; Nakashima, H.; Shimamura, M.; Inayama, S.; Fujiwara, T.; Takeuchi, Y.; Uehara, Y.; Kirk, K. L.; Nakata, E.; Hori, H. *Bioorg. Med. Chem.* **2008**, *16*, 6042.
10. Mallia, M. B.; Mathur, A.; Subramanian, S.; Banerjee, S.; Sarma, H. D.; Venkatesh, M. *Bioorg. Med. Chem. Lett.* **2005**, *15*, 3398.
11. Born, J. L.; Smith, B. R.; Harper, N.; Koch, C. J. *Biochem. Pharmacol.* **1992**, *43*, 1337.
12. Brown, J. M. *Int. J. Radiat. Oncol. Biol. Phys.* **1989**, *16*, 987.
13. Lord, E. M.; Harwell, L.; Koch, C. J. *Cancer Res.* **1993**, *53*, 5721.
14. Webster, L. T. Drugs Used in the Chemotherapy of Protozoal Infections. In *The Pharmacological Basis of Therapeutics*; Gilman, A., Rall, T. W., Nies, A. S., Taylor, P., Eds., 8th ed.; Pergamon Press: New York, 1990; pp 999–1007.
15. Alvaro, R. F.; Wislocki, P. G.; Miwa, G. T.; Lu, A. Y. *Chem. Biol. Interact.* **1992**, *82*, 21.
16. Chapman, J. D. *N. Eng. J. Med.* **1979**, *301*, 1429.
17. Swenson, D. H.; Laster, B. H.; Metzger, R. L. *J. Med. Chem.* **1996**, *39*, 1540.
18. Wang, Z.-M.; Kolb, H. C.; Sharpless, K. B. *J. Org. Chem.* **1994**, *59*, 5104.
19. Meydan, N.; Grunberger, T.; Dadi, H.; Shahar, M.; Arpaia, E.; Lapidot, Z.; Leeder, J. S.; Freedman, M.; Cohen, A.; Gazit, A.; Levitzki, A.; Roifman, C. M. *Nature* **1996**, *379*, 645.
20. Mariano, C.; Marder, M.; Blank, V. C.; Roguin, L. P. *Bioorg. Med. Chem.* **2006**, *14*, 2966.
21. Han, C. K.; Ahn, S. K.; Choi, N. S.; Hong, R. K.; Moon, S. K.; Chun, H. S.; Lee, S. J.; Kim, J. W.; Hong, C. I.; Kim, D.; Yoon, J. H.; No, K. T. *Bioorg. Med. Chem. Lett.* **2000**, *10*, 39.
22. Dallavalle, S.; Cincinelli, R.; Nannei, R.; Merlini, L.; Morini, G.; Penco, S.; Pisano, C.; Vesci, L.; Barbarino, M.; Zuco, V.; Cesare, M. D.; Zunino, F. *Eur. J. Med. Chem.* **2009**, *44*, 1900.
23. Davis, R.; Kumar, N. S.; Abraham, S.; Suresh, C. H.; Rath, N. P.; Tamaoki, N.; Das, S. *J. Phys. Chem. C* **2008**, *112*, 2137.
24. Sheldrick, G. M.. SHELX-97. In *Program for X-ray Crystal Structure Solution and Refinement*; Göttingen University: Germany, 1997.
25. Tsou, H. R.; Mamuya, N.; Johnson, B. D.; Reich, M. F.; Gruber, B. C.; Ye, F.; Nilakantan, R.; Shen, R.; Discafani, C.; DeBlanc, R.; Davis, R.; Koehn, F. E.; Greenberger, L. M.; Wang, Y. F.; Wissner, A. *J. Med. Chem.* **2001**, *44*, 2719.